Order-disorder phase transition of vacancies in surfaces: The case of Sn/Cu(001)-0.5 ML

J. E. Gayone,[1] A. Carrera,[1] O. Grizzi,[1] S. Bengió,[1] E. A. Sánchez,[1] J. Martínez-Blanco,[2] E. G. Michel,[2] J. D. Fuhr,[1] and H. Ascolani[1]

[1]*Centro Atómico Bariloche, CNEA, and CONICET, Av. E. Bustillo 9500, R8402AGP Bariloche, Argentina*

[2]*Departamento de Física de la Materia Condensada and Instituto Universitario de Ciencia de Materiales "Nicolás Cabrera," Universidad Autónoma de Madrid, 28049 Madrid, Spain*

(Received 31 May 2010; published 15 July 2010)

We investigate the structural phase transition $(3\sqrt{2}\times\sqrt{2})R45° \leftrightarrow (\sqrt{2}\times\sqrt{2})R45°$ of 0.5 ML Sn/Cu(001) using a combination of scanning tunneling microscopy, time-of-flight direct-recoil spectroscopy, and Monte Carlo simulations. Cu vacancies are observed for both phases. At low temperature, Cu vacancies are ordered in a regular array of lines. At high temperature, Sn atoms occupy similar adsorption sites as at low temperature but Cu vacancies are disordered. We conclude that the atomistic mechanism behind the structural phase transition is an order/disorder transition driven by the Cu-vacancy entropy.

DOI: 10.1103/PhysRevB.82.035420 PACS number(s): 68.35.Rh, 68.37.Ef, 68.47.De, 68.49.−h

I. INTRODUCTION

Atomic vacancies are an essential ingredient of many technologically interesting multicomponent materials. We may mention their role in surface catalysis[1] or phase-change materials.[2] Ordered vacancy sublattices in the ground state are important because of the strong impact on the physical properties of the material.[3] The case of two dimensions (2D) is specially attractive, as the correlation between vacancy ordering and physical properties is more evident. A good example is that of several known instances of order/disorder phase transitions involving vacancies.[4–6]

The deposition of 0.5 monolayers (MLs) of Sn on Cu(001) produces, at room temperature, a single-layer surface alloy with $(3\sqrt{2}\times\sqrt{2})R45°$ (hereafter $3\sqrt{2}$) periodicity. The superstructure is due to the existence of lines of Cu vacancies, with a Sn:Cu surface stoichiometry of 3:2.[7–9] The $3\sqrt{2}$ phase undergoes a temperature-induced reversible crystallographic transition to a $(\sqrt{2}\times\sqrt{2})R45°$ (hereafter $\sqrt{2}$) phase at 360 K as observed by low-energy electron diffraction (LEED).[10] The structural transition is accompanied by an electronic transition, compatible with a condensation of a charge-density wave (CDW),[11,12] which was proposed as an important driving force of the $3\sqrt{2}\leftrightarrow\sqrt{2}$ phase transition.[10,13] Yaji *et al.* have recently found evidence of order/disorder behavior.[14] This feature is not incompatible with a CDW scenario[11] but it indicates that the dynamics of the phase transition is more complex than initially thought. The fact that the $3\sqrt{2}$ structure is formed by lines of ordered Cu vacancies suggests that their specific role should be analyzed.

In this work, we report a temperature-induced 2D phase transition where the role of vacancies is monitored at atomic level. Using a combination of experimental techniques and Monte Carlo (MC) simulations, we analyze the structural properties of the $3\sqrt{2}\leftrightarrow\sqrt{2}$ phase transition. Scanning tunneling microscopy (STM) images provide us with real-space information on both phases. We exploit the well-known applicability of direct-recoiling spectroscopy (DRS) for studying surface alloys and surfaces with vacancy lines[15] in order to monitor the Cu vacancies as a function of temperature. Combining this technique with MC simulations, we conclude that the high-temperature (HT) phase is disordered. The phase transition is described as the ordering of Cu vacancies at low temperature.

II. EXPERIMENTAL DETAILS

DRS is a technique derived from ion-scattering spectroscopy with high sensitivity to the top surface layer.[16] Briefly, it is based on the detection, at a fixed forward emission angle, of the fast recoiling target atoms produced by kiloelectron volt ion projectiles to obtain information about the elemental composition and the atomic structure of the top atomic layers of a surface. The elemental composition of the surface is derived from the energy analysis of the surface atoms emitted in single collisions with the primary beam while the surface atomic structure is derived from the variation in the recoil intensity with the incident direction of the ions. Each target atom modifies the ion and recoil trajectories in a surface region on the order of 1 $Å^2$ resulting in strong shadowing and blocking effects that are characteristic of the collision partners and of the surface geometry. In particular, these shadowing and blocking effects are mainly governed by the distance between the nearest-neighbor atoms so there is no need of long-range order in order to observe crystallographic effects on the recoil intensity. Finally, the detection of both recoiling ions plus neutrals by time-of-flight (TOF) methods avoids dealing with neutralization effects and reduces the ion bombardment dose producing negligible damage.

The preparation of the 0.5 ML Sn/Cu(001) surface has been described before.[8] Two ultrahigh-vacuum chambers were used. The first one is equipped with a variable-temperature STM (Omicron) and LEED. The DRS measurements are carried out in the second chamber, also equipped with LEED.[17] All DRS spectra were acquired with a 5 keV $^{20}Ne^{+}$ ion-pulsed beam and fixed scattering angle (δ=30°). The Cu(001) substrate was prepared in this case by grazing Ar sputtering (20 keV, 2° incidence with respect to the surface plane) and annealing to 720 K. During sputtering the sample was kept under continuous rotation around its normal in order to change the azimuthal incidence angle. This pro-

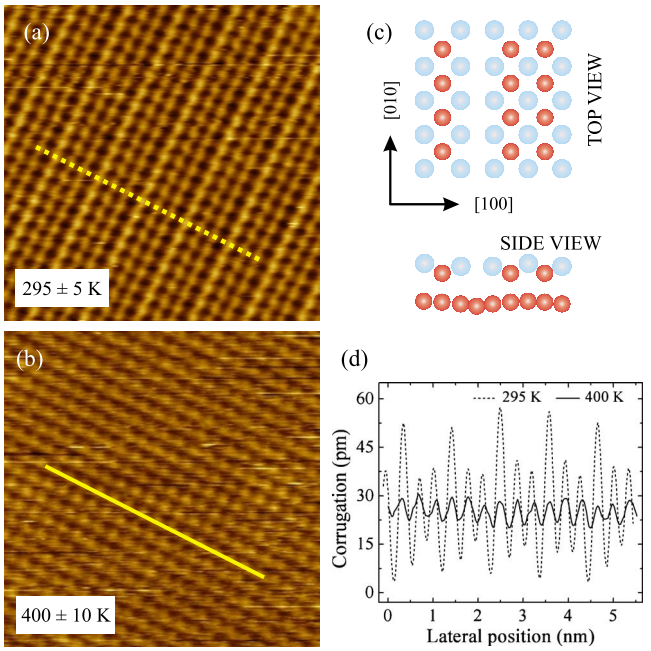

FIG. 1. (Color online) Experimental filled-state STM images (70×70 Å^2, $V=-0.05$ V, $I=2$ nA) for (a) $3\sqrt{2}$ and (b) $\sqrt{2}$ phases obtained at 295 K and 400 K, respectively. (c) Schematic of the vacancy-line model for the $3\sqrt{2}$ phase. (d) Vertical profiles corresponding to the $3\sqrt{2}$ and $\sqrt{2}$ phases, as highlighted on the images.

cedure was very effective to smooth out the initial surface roughness[18,19]

III. RESULTS

A. STM

Figures 1(a) and 1(b) show typical filled-state STM images of the low-temperature (LT) and HT phases, respectively, while Fig. 1(d) shows height profiles for both phases. The protrusions in the image of Fig. 1(a) correspond to Sn atoms arranged in a rectangular lattice, with a $3\sqrt{2}$ periodicity along the [100] direction [Fig. 1(c)].[8] The corresponding height profile [Fig. 1(d)] shows that one out of three Sn atoms has an apparent height ~10 pm larger than the other two atoms, which are deeper and dimerized, as a consequence of the formation of the Cu-vacancy line.

Accordingly, protrusions in the HT image are also assigned to Sn atoms. The protrusions all look equivalent and are arranged in a $(\sqrt{2}\times\sqrt{2})R45°$ lattice, with a strong reduction in the total vertical corrugation [Fig. 1(d)] from ~50 pm in the LT phase to ~10 pm at HT. The two characteristic features of the LT phase image, corrugation and dimerization with $3\sqrt{2}$ periodicity, are not observed in the HT phase image. Two possible models for the HT phase are compatible with the observed STM image and LEED experiments:[10,20] (i) an ordered $(\sqrt{2}\times\sqrt{2})R45°$ surface alloy or overlayer, free of Cu vacancies; or (ii) a disordered surface alloy with Cu vacancies diffusing faster than the STM scanning speed.

B. TOF-DRS

Figure 2(a) shows a set of TOF-DRS spectra acquired for

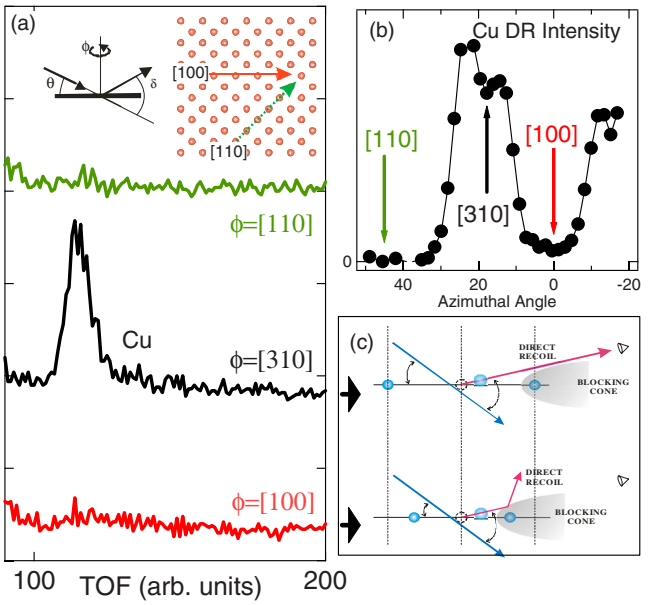

FIG. 2. (Color online) (a) TOF spectra for the clean Cu(001) surface for $\theta=20°$ and for different azimuthal angles ϕ. The inset shows the definition of the angles ϕ and θ and a schematic of the Cu(001) surface. (b) Cu direct-recoil intensity (peak area) vs azimuthal angle for $\theta=20°$. (c) Schematic of the blocking effect.

the clean Cu(001) surface at different azimuthal incident angles ϕ for a fixed polar incidence angle ($\theta=20°$). For a definition of the angles, see Fig. 2(a) (inset). The peak observed for ϕ along the [310] crystallographic direction corresponds to the Cu atoms recoiled into the scattering angle $\delta=30°$ coming from single collisions with the primary beam. The peak is only observed at certain azimuthal directions, as shown in Fig. 2(b). At this incident polar angle, the detector is at a small emission angle measured from the surface so that the large variation in the peak intensity with ϕ is determined mainly by blocking effects on the outgoing trajectory of the Cu recoils [see Fig. 2(c)]. Along the compact azimuthal directions, where the distance d between two consecutive surface atoms is smaller, the trajectory of the emitted surface Cu atoms intersects the blocking cone of its neighbor atom. As it deviates from its straight trajectory to the detector, no peak is observed in the spectrum in this case. Setting the azimuthal angle away from the principal directions increases d. The recoiling atom can then reach the detector and the intensity of the peak increases. The blocking effects explain the strong minima observed in the curve of the direct-recoil Cu intensity vs ϕ along the more compact [100] and [110] azimuthal directions. Notice that the deepest minimum corresponds to the most compact [110] direction.

Figure 3(a) shows a set of TOF spectra measured for the Sn/Cu interface (full lines) with the same scattering geometry as in Fig. 2(a). The clean surface spectrum for $\phi=[100]$ is included as a reference (dotted line). After adsorbing 0.5 ML of Sn, a Cu DR peak appears for $\phi=[100]$. Clearly, neither emission of adatoms nor atoms from steps can explain the peak because it vanishes from the [100] azimuthal direction, as shown in the two top spectra of Fig. 3(a) and in Fig. 3(b). The appearance of the Cu DR peak is thus a

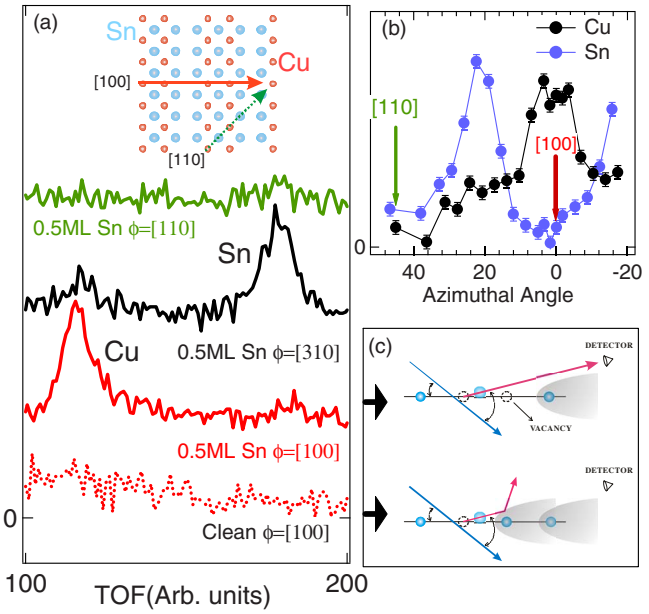

FIG. 3. (Color online) (a) TOF spectra for the $3\sqrt{2}$ phase (full lines) and for the clean surface (dotted line). The inset shows a schematic of the vacancy-line model for the $3\sqrt{2}$ phase. (b) Cu and Sn recoiling intensities as a function of the azimuthal angle measured at $\theta=20°$. (c) Schematic of the blocking effect.

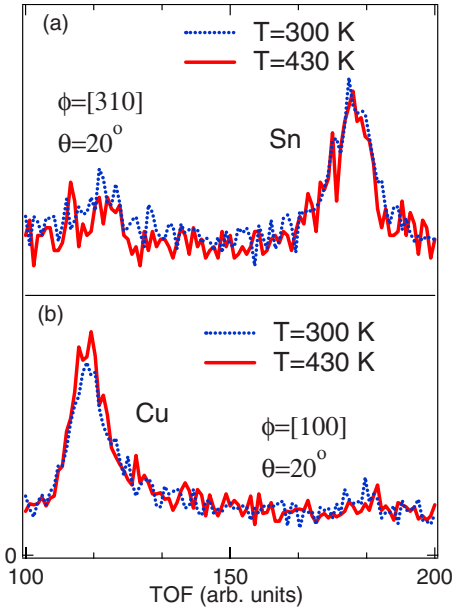

FIG. 4. (Color online) (a) TOF spectra for the $3\sqrt{2}(T=300$ K) and the $\sqrt{2}(T=430$ K) phase measured at ($\theta=20°$, $\phi=[100]$) (b) TOF spectra for the $3\sqrt{2}(T=300$ K) and the $\sqrt{2}(T=430$ K) phase measured at ($\theta=20°$, $\phi=[310]$).

characteristic feature of the $3\sqrt{2}$ phase. The fact that the Cu DR intensity has a maximum along the [100] azimuthal direction shows that the trajectory of the Cu DR is not deviated by the blocking cone of its neighboring atom [see the schematic drawing in Fig. 3(c)]. This means that the distance between two consecutive surface Cu atoms along the [100] azimuthal direction must necessarily be larger than on the clean Cu(001) surface. This effect is fully consistent with the Cu-vacancy-line model. We therefore conclude that the area of the DR peak [second spectrum from the bottom in Fig. 3(a)] is proportional to the number of detectable Cu atoms that have an atom vacancy in the next-neighbor site along the beam direction (N_{vCu}).

The intensity variation in the Sn DR peak with azimuthal angle in Fig. 3(b) is similar to the one of the Cu DR peak on the clean Cu(001) surface. However, in the case of the Sn DR peak, the deepest minimum is along the [100] direction, instead of the [110], indicating that the [100] direction is the most compact from the point of view of the DRS technique and that the Sn atoms are arranged in a squared lattice rotated 45° with respect to the 1×1 unit cell as expected according to the vacancy-line surface-alloy structure.[21]

Figures 4(a) and 4(b) show the HT phase spectra measured along $\phi=[310]$ and $\phi=[100]$, respectively, together with the corresponding LT phase spectra. There are no significant changes in temperature in the intensity of both the Sn and Cu recoils. This result, combined with the STM image of the HT phase, indicates that at high T, the positions of Sn atoms are on average the same as in the LT phase. As for the LT case, the Cu DR peak observed at 430 K in Fig. 4(b) is proportional to N_{vCu}, and can be used to monitor the vacancies across the phase transition. From the comparison with the Cu DR peak measured at 300 K, it follows that there is a small increase in N_{vCu} at 430 K. This result indicates that most of the vacancies remain on the HT phase. We therefore discard the possibility that all Cu vacancies are filled at the $\sqrt{2}$ phase.

C. MC simulations

In order to gain more insight into the nature of the transition, we performed canonical Monte Carlo simulations. We assumed a $(\sqrt{2}\times\sqrt{2})R45°$ arrangement of Sn atoms while the remaining sites in the outermost surface layer form a grid where each site (i,j) can be occupied either by a Cu atom ($n_{i,j}=1$) or by a vacancy ($n_{i,j}=0$). We described the effective on-site energy and lateral interactions, between Cu atoms forming the surface alloy, by a first-principles lattice-gas Hamiltonian (LGH).[22] We fitted the ten parameters of the LGH (E_0, V_1^p, V_2^p, V_3^p, V_4^p, V_1^t, V_2^t, V_3^t, V_6^t, and V_2^q in the nomenclature of Ref. 22), using a set of *ab initio* total-energy calculations,[8] consisting of 18 totally relaxed vacancy configurations in unit cells up to (3×3) of the corresponding $\sqrt{2}$ unit cell. The total-energy calculations were performed using the QUANTUM-ESPRESSO package.[23] We model the Cu(001) surfaces using periodic seven-layer slabs with the two bottom layers fixed at the theoretical bulk value 1.815 Å and a vacuum region of 10.89 Å. We used the generalized-gradient approximation as given by the PW91 functional[24] for the exchange-correlation term, a wave-function/charge cutoff of 25/200 Ry, and for the Brillouin integrations a $15\times15\times1$ grid of k points for the $\sqrt{2}$ unit cell, and equivalent grids for the larger unit cells.

For the MC simulations, we used a grid with $N_s=3600(=60\times60)$ sites. Each elementary MC step consists of a switch in the occupancy between two random sites i and j. We used $10^5\times N_s$ MC passes for equilibration, followed by

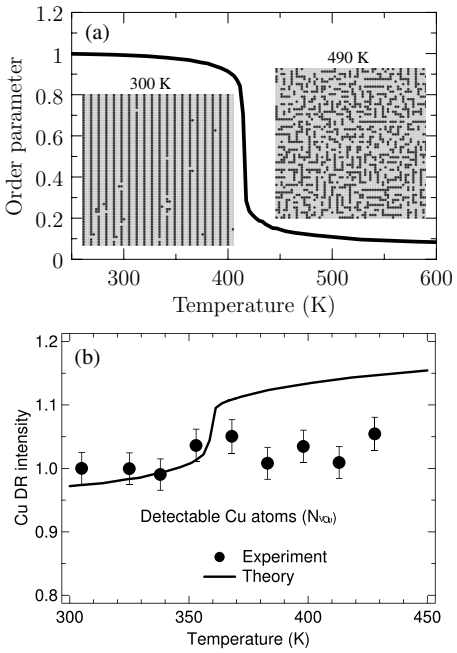

FIG. 5. (a) Experimental and calculated N_{vCu}. (b) Simulated order parameter vs temperature and two snapshots of the MC simulations representative of the low- and high-temperature phases. Light and dark gray spots correspond to grid sites occupied by a Cu atom or a vacancy, respectively.

another $10^5 \times N_s$ passes for averaging. The order of the system was characterized by an order parameter $\eta = \frac{3}{2}\sum_{\substack{\alpha,\beta=0 \\ \alpha<\beta}}^{2} |M_\alpha - M_\beta|$, with

$$M_\alpha = \frac{1}{N_s}\left[\sum_{\substack{i,j \\ i \bmod 3=\alpha}} n_{i,j} + \sum_{\substack{i,j \\ j \bmod 3=\alpha}} n_{i,j} \right],$$

N_s being the number of sites in the grid. This order parameter takes the value $\eta=1$ ($\eta=0$) for the totally ordered (disordered) phase.

Figure 5(a) shows the evolution of the order parameter η with temperature and two snapshots of the MC simulations representative of the low- and high-temperature phases. In the snapshots, light and dark gray spots correspond to grid sites occupied by a Cu atom or a vacancy, respectively. The evolution of the order parameter depicts an order-disorder transition with a critical temperature of $T_c \simeq 416$ K, which is close to the experimental value of $T_c \simeq 360$ K.[10] In the first snapshot, we can see that even at this low temperature (more than 100 K below the transition temperature) there is some degree of disorder. On the other hand, in the high-temperature snapshot, we can see small dark segments that correspond to an alignment of vacancies, showing that correlations between the vacancies remain above the transition temperature.

In order to compare the MC simulations with the present TOF-DRS measurements, in Fig. 5(b) we show the evolution of the experimental and calculated N_{vCu} with temperature. In this figure, the temperature scale of the simulations has been rescaled in order to have $T_c=360$ K. A small increase of $\sim 5\%$ in the experimental N_{vCu} is detected when crossing the phase transition. This value is only slightly above our experimental error (4%). In the case of the calculated N_{vCu}, at T_c we can see a jump of $\gtrsim 10\%$ in the calculated N_{vCu}, which comes from the disordering of the vacancies. In the ordered phase, and taking into account both domains, only 1/4 of Cu atoms have a vacancy as neighbor in the ion-beam incident direction. On the other hand, in the limit of totally disordered vacancies, this fraction is 1/3, i.e., an increase of 33% should be observed in N_{vCu} if the transition occurs from a fully ordered to a fully disordered case. The smaller increase observed for the simulated N_{vCu} is traced back to the correlations between vacancies, which remain above T_c in the MC simulation. From the good agreement between the MC simulation and experimental temperature dependence of N_{vCu}, we conclude that the transition is of an order/disorder type, with the number of vacancies remaining mainly constant across T_c.

IV. CONCLUSIONS

The results reported in this work constitute direct evidence for the existence of Cu vacancies in the outermost layer of both the LT and the HT phases of the 0.5 ML Sn/Cu(001) surface alloy. This evidence demonstrates convincingly that the $(\sqrt{2}\times\sqrt{2})R45°$ HT phase is disordered, with the positions of the Sn atoms, on average, being similar to the corresponding positions at LT while the Cu vacancies form a 2D gas. In this context, the collapse of the electronic gap of the surface state at 400 K reported in Ref. 10 could be explained by the reduction in the characteristic length of the $3\sqrt{2}$ domains below the coherent length of the S_2 surface state (see Fig. 4 in Ref. 8). Moreover, the fact that the gap size (0.7 eV) is a factor 23 larger than kT_c, strongly suggests that the configurational entropy of the partially filled sublayer of Cu atoms is the main driving force of the transition.

The atomistic mechanism of the $(3\sqrt{2}\times\sqrt{2})R45° \leftrightarrow (\sqrt{2}\times\sqrt{2})R45°$ crystallographic phase transition can therefore be characterized as an order-disorder transition driven by the Cu vacancies entropy. Therefore, this surface alloy is a model system presenting a 2D order-disorder structural transition that induces an electronic transition. The study and further research of this interface will shed light on our understanding of a range of related phase transitions.[5,6,13,25]

ACKNOWLEDGMENTS

We acknowledge financial support by the following Argentine institutions: ANPCYT (Grants No. PICT2005/33432, No. PICT2006/715, and No. PME2003/118), ANTORCHAS Foundation, CONICET (Grant No. PIP2009/112-200801-00958), and UNCuyo (Grants No. 06/C323 and No. 06/C317). We also acknowledge financial support from the Spanish MICINN (Grants No. FIS2008-00399 and No. FIS2007-29085-E). We thank Linda Yael for English revision.

[1] T. Mitsui, M. K. Rose, E. Fomin, D. F. Ogletree, and M. Salmeron, Nature (London) **422**, 705 (2003).
[2] M. Wuttig, D. Lüsebrink, D. Wamwangi, W. Welłnic, M. Gilleßen, and R. Dronkowski, Nature Mater. **6**, 122 (2007).
[3] O. Dulub, M. Batzill, S. Solovev, E. Loginova, A. Alchagirov, T. E. Madey, and U. Diebold, Science **317**, 1052 (2007).
[4] C. Jiang, Phys. Rev. B **78**, 064206 (2008).
[5] H. Iddir, D. D. Fong, P. Zapol, P. H. Fuoss, L. A. Curtiss, G.-W. Zhou, and J. A. Eastman, Phys. Rev. B **76**, 241404(R) (2007).
[6] T. Nakagawa, O. Ohgami, Y. Saito, H. Okuyama, M. Nishijima, and T. Aruga, Phys. Rev. B **75**, 155409 (2007).
[7] J. Martínez-Blanco, V. Joco, C. Quirós, P. Segovia, and E. G. Michel, J. Phys.: Condens. Matter **21**, 134011 (2009).
[8] J. D. Fuhr, J. E. Gayone, J. Martínez-Blanco, E. G. Michel, and H. Ascolani, Phys. Rev. B **80**, 115410 (2009).
[9] K. Pussi, E. AlShamaileh, E. McLoughin, A. A. Cafolla, and M. Lindroos, Surf. Sci. **549**, 24 (2004).
[10] J. Martínez-Blanco, V. Joco, H. Ascolani, A. Tejeda, C. Quirós, G. Panaccione, T. Balasubramanian, P. Segovia, and E. G. Michel, Phys. Rev. B **72**, 041401(R) (2005).
[11] E. Tosatti, in *Electronic Surface and Interface States on Metallic Systems*, edited by E. Bertel and M. Donath (World Scientific, Singapore, 1995).
[12] G. Grüner, *Density Waves in Solids* (Addison-Wesley, Reading, MA, 1994).
[13] T. Aruga, Surf. Sci. Rep. **61**, 283 (2006).
[14] K. Yaji, Y. Nara, K. Nakatsuji, T. Iimori, K. Yagyu, R. Nakayama, N. Nemoto, and F. Komori, Phys. Rev. B **78**, 035427 (2008).
[15] F. Masson and J. W. Rabalais, Surf. Sci. **253**, 245 (1991).
[16] J. W. Rabalais, *Principles and Applications of Ion Scattering Spectrometry: Surface Chemical and Structural Analysis* (Wiley-Interscience, New Jersey, 2003).
[17] L. N. Serkovic Loli, E. A. Sánchez, J. E. Gayone, O. Grizzi, and V. A. Esaulov, Phys. Chem. Chem. Phys. **11**, 3849 (2009).
[18] J. E. Gayone, R. G. Pregliasco, G. R. Gomez, E. A. Sánchez, and O. Grizzi, Phys. Rev. B **56**, 4186 (1997).
[19] L. M. Rodríguez, J. E. Gayone, E. A. Sánchez, H. Ascolani, O. Grizzi, M. Sánchez, B. Blum, G. Benitez, and R. C. Salvarezza, Surf. Sci. **600**, 2305 (2006).
[20] J. Martínez-Blanco, V. Joco, P. Segovia, T. Balasubramanian, and E. G. Michel, Appl. Surf. Sci. **252**, 5331 (2006).
[21] Although the vacancy-line model is a surface-alloy structure, the Cu atoms in the top surface layer are expected to play a minor role due to the fact that they are located at a slightly lower height than the Sn atoms.
[22] Y. Zhang, V. Blum, and K. Reuter, Phys. Rev. B **75**, 235406 (2007).
[23] P. Giannozzi *et al.*, J. Phys.: Condens. Matter **21**, 395502 (2009).
[24] J. P. Perdew, J. A. Chevary, S. H. Vosko, K. A. Jackson, M. R. Pederson, D. J. Singh, and C. Fiolhais, Phys. Rev. B **46**, 6671 (1992).
[25] V. Joco, J. Martínez-Blanco, P. Segovia, T. Balasubramanian, J. Fujii, and E. G. Michel, Surf. Sci. **600**, 3851 (2006).